$$= \int_0^\infty \text{prob}\,(A|\mu,\text{centric})\,\text{prob}\,(\mu|\text{centric})\text{d}\mu. \quad (A11)$$

With the MaxEnt assignment of ($A7$) and a Jeffreys prior for prob (μ|centric), because the knowledge that a reflection is centric says nothing about its expected value, the integral of ($A11$) yields

$$\text{prob}\,(A|\text{centric}) \propto 1/A, \quad \text{for } A > 0. \quad (A12)$$

Equation ($A12$) is, of course, equivalent to ($A10$) with a change of variables.

In conclusion, it can be seen that the Wilson distributions can easily be derived with the maximum-entropy principle. The acentric case arises from the imposition of a constraint on the expected value of the intensity of a general reflection, whereas the centric p.d.f. requires the additional knowledge that the structure factor must be real. If there is complete uncertainty as to the absolute scale of the data then, as expected, both the Wilson distributions revert to the form of the Jeffreys prior.

References

ANTONIADIS, A., BERRUYER, J. & FILHOL, A. (1990). *Acta Cryst.* A**46**, 692–711.

BRICOGNE, G. (1991). *Acta Cryst.* A**47**, 803–829.

DAVID, W. I. F. (1987). *J. Appl. Cryst.* **20**, 316–319.

DAVID, W. I. F. (1990). *Nature (London)*, **346**, 731–734.

ESTERMANN, M. A., MCCUSKER, L. B. & BAERLOCHER, C. (1992). *J. Appl. Cryst.* **25**, 539–543.

FRENCH, S. & WILSON, K. (1978). *Acta Cryst.* A**34**, 517–525.

GILMORE, C. G., HENDERSON, K. & BRICOGNE, G. (1991). *Acta Cryst.* A**47**, 830–841.

JANSEN, J., PESCHAR, R. & SCHENK, H. (1992). *J. Appl. Cryst.* **25**, 231–236, 237–243.

JAYNES, E. T. (1983). *Papers on Probability, Statistics and Statistical Physics*, edited by R. D. ROSENKRANTZ. Dordrecht: Reidel.

JEFFREYS, H. (1939). *Theory of Probability*. Oxford Univ. Press.

LE BAIL, A., DUROY, H. & FOURQUET, J. L. (1988). *Mater. Res. Bull.* **23**, 447–452.

NELDER, J. A. & MEAD, R. (1965). *Comput. J.* **7**, 308–313.

OATLEY, S. & FRENCH, S. (1982). *Acta Cryst.* A**38**, 537–549.

PAWLEY, G. S. (1981). *J. Appl. Cryst.* **14**, 357–361.

PRESS, W. H., FLANNERY, B. P., TEUKOLSKY, S. A. & VETTERLING, W. T. (1986). *Numerical Recipes: the Art of Scientific Computing*. Cambridge Univ. Press.

WILSON, A. J. C. (1949). *Acta Cryst*, **2**, 318–321.

Acta Cryst. (1994). A**50**, 714–725

A Topological Definition of a Wigner–Seitz Cell and the Atomic Scattering Factor

BY P. F. ZOU AND R. F. W. BADER

Department of Chemistry, McMaster University, Hamilton, Ontario L8S 4M1, Canada

(*Received* 4 *January* 1994; *accepted* 6 *April* 1994)

Abstract

An atom is defined as a region of space bound by a surface of local zero flux in the gradient vector field of the electron density. The same boundary condition defines a proper open system, one whose observables and their equations of motion are defined by quantum mechanics. Applied to a crystal, this boundary condition coincides with the original definition of the atomic cell in metallic sodium given by Wigner & Seitz. It is proposed that it be used to generalize the concept of a Wigner–Seitz cell, defining it as the smallest connected region of space bounded by a 'zero-flux surface' and exhibiting the translational invariance of the crystal. This definition, as well as removing the arbitrary nature of the original method of construction of the cell in the general case, maximizes the relation of the cell and the derived atomic form factors to the physical form exhibited by the charge distribution of its constituent atoms. The topology of the electron density, as summarized in terms of its critical points, also defines the atomic connectivity and structure within a cell. Attention is drawn to the correspondence of the symmetries of the structural elements determined by the critical points with the site symmetries tabulated in *International Tables for Crystallography*. The atomic scattering factor is defined for an atom in a crystal and determined in *ab initio* calculations for diamond and silicon. The transferable nature of atomic charge distributions is demonstrated. It enables one to estimate a structure factor and its phase in a crystal using the density of an atom or functional group obtained in a molecular calculation. Atoms in a crystal, along with defects and vacancies, are identifiable with bounded regions of real space. Their properties are additive and are defined by quantum mechanics.

1. Introduction

The amplitudes of X-rays scattered by a crystal are determined by the electronic charge distribution. Two essential concepts are involved in the interpreta-

tion of the scattering patterns and their intensities obtained for a crystal: the translational invariance of the unit cell and the atom as the source of the scattering. Atomic scattering factors are used to make a comparison between the observed intensities and those calculated from an assumed arrangement of the nuclei in a crystal structure determination. Conventionally, the charge distribution of an atom in a crystal is taken to be that of a spherical isolated atom or that of a model refined from the isolated atom. This paper is concerned with the definition of a scattering factor for an atom in a crystal in a manner that preserves the translational invariance and space-filling properties of the Wigner–Seitz cell. This is achieved by proposing a generalization of the definition of a Wigner–Seitz cell to reflect the dominant topological property of the charge distribution, one which coincides with the variational definition of a quantum subsystem.

As early as 1915, Bragg stressed that the understanding of the scattering of X-rays by a crystal necessitated taking into account the effect of the distribution of electrons over a region whose dimensions are comparable with the wavelength of the radiation employed, that is, an atomic dimension (Bragg, 1915). He later made the following statement relating to the then recently observed 222 reflection in the diamond structure, which is forbidden by the spherical-atom model (Bragg, 1921): 'It is necessary, therefore, to suppose that the attachment of one atom to the next is due to some directed property, and the carbon atom has four such special directions: as indeed the tetravalency of the atom might suggest.' Later experimental work did indeed verify the existence of the tetrahedral nature of the atomic charge distributions in the diamond structure, studies that, along with those on silicon (Göttlicher & Wölfel, 1959; Dawson, 1967), were the forerunners of the experimental determination of the charge density by accurate X-ray diffraction methods, as recently summarized by Jeffrey & Piniella (1991).

The requirements for obtaining a physically and mathematically unique decomposition of the charge distribution of a crystal into its atomic components, one which determines the atomic symmetries and their associated directed properties, are given in § 2. These considerations lead one to conclude that an atom in a crystal should be defined in the same manner as an atom in a molecule: as a region of space bounded by a surface of zero flux in the gradient vector field of the electronic charge density (Bader & Beddall, 1972; Bader, 1990). Further sections apply the topological theory of molecular structure to the electron distribution in a crystal and apply the concept of an atom in a crystal to the definition and calculation of atomic form factors, with particular applications to diamond and silicon.

Charge distributions of diamond and silicon and of the related zincblende structures BN, BP and AlP were calculated using the program *CRYSTAL* (Pisani, Dovesi & Roetti, 1988), a Hartree–Fock procedure for an infinite lattice, using a Gaussian basis set of the form 6-21G, augmented with a set of *d* functions (Binkley, Pople & Hehre, 1980; Pisani, Dovesi & Orlando, 1992). The topological analysis of the charge distribution and the properties of atoms in a crystal were obtained using suitably modified versions of the corresponding programs for atoms in molecules (Biegler-König, Bader & Tang, 1982.

2. Atoms in crystals

Any decomposition of the space of a crystal that preserves the translational invariance of the lattice and that exhausts all of space is a mathematically acceptable partitioning. Physically, however, and from the point of view of imposing boundary conditions in solving Schrödinger's equation for a periodic lattice, further constraints are required. This is exemplified in the classic study of metallic sodium by Wigner & Seitz (1933), who accomplished these goals by being the first to define an atom in a crystal. To obtain the wave function for the single valence electron in each Na atom in this body-centred-cubic crystal, they satisfied both the mathematical and physical requirements by surrounding each nucleus (in this case, each lattice point) by a space-filling polyhedron that had the additional desirable property of reflecting the local symmetry of the cubic point group. This was done by constructing planes at the midpoints of and perpendicular to the lines linking one nucleus to its two sets of equivalent neighbours. Because of the translational symmetry of the crystal, the derivative of the ground-state wave function of a free electron must vanish perpendicular to each plane of the resulting 14-sided polyhedron representing the crystalline Na atom, the condition $\nabla\psi \cdot \mathbf{n} = 0$. These atomic polyhedra generate the unit cell that most closely approximates a sphere and Wigner & Seitz imposed the boundary condition that $\partial\psi/\partial r = 0$ at the surface of the sphere of equal volume in obtaining the solutions to the radial wave equation for a spherically symmetric potential. Slater (1934) later extended the method of Wigner & Seitz to take into account the actual shape of the crystal polyhedra.

For the nodeless one-electron ground-state wave function, the periodic boundary condition satisfied by the polyhedral Wigner–Seitz cell, and indeed the condition defining the cell, can be alternatively stated in terms of the electron density $\rho(\mathbf{r})$ as

$$\nabla\rho(\mathbf{r}) \cdot \mathbf{n}(\mathbf{r}) = 0 \quad \forall\, \mathbf{r} \in S(\mathbf{r}), \tag{1}$$

where $\mathbf{n}(\mathbf{r})$ is the unit vector normal to $S(\mathbf{r})$, the

surface of the cell. A region of space bounded by surfaces that locally satisfy this condition of exhibiting a zero-flux in $\nabla\rho$ is also the definition of an atom in a molecule (Bader & Beddall, 1972; Bader, 1990), where $\rho(\mathbf{r})$ is, in general, the charge density of an N-electron system

$$\rho(\mathbf{r}) = N\int \mathrm{d}\tau' \psi^*\psi. \qquad (2)$$

The integration symbol $\int \mathrm{d}\tau'$ in (2) implies a summation over all spin coordinates and the integration over the spatial coordinates of all electrons but one, whose coordinate is denoted **r**. This zero-flux surface condition leads to an exhaustive partitioning of the space of any system into a collection of mononuclear, *i.e.* atomic, fragments because of the dominant topological property exhibited by the electronic charge distribution – that, in general, it exhibits local maxima only at the positions of the nuclei (Fig. 1*a*) (Bader, 1990; Bader, Nguyen-Dang & Tal, 1981). As a consequence, a nucleus acts as the terminus for the paths of the gradient vectors of ρ that traverse its basin, leading to the definition of an atom as the union of a nucleus and its basin. The basin is separated from the basins of neighbouring atoms by zero-flux surfaces (Fig. 1*b*). This definition applies to a free atom or to an atom bound in a molecule or in a crystal.

An atom in a molecule or a crystal is an open system in that it can exchange charge and momentum across its interatomic surfaces. It is, therefore, equally important that (1) is found to be the boundary condition for the definition of a proper open system (Bader & Nguyen-Dang, 1981; Bader, 1990) using Schwinger's (1951) variational principle of stationary action. They are termed *proper* since only the observables for such open systems are described by the correct equations of motion (Bader, 1994).

The expectation values of all observables are defined for a proper open system and the associated equations of motion yield the theorems governing their behaviour (Bader & Nguyen-Dang, 1981; Bader, 1990). For each choice of observable denoted $\hat{G}$, the generator of a corresponding change in the action, one obtains an atomic theorem: setting $\hat{G}$ equal to an electronic momentum operator $\hat{\mathbf{p}}$ yields the atomic force theorem and an equation of motion for an open system; setting $\hat{G}$ equal to the product of electronic position and momentum operators $\hat{\mathbf{r}}\cdot\hat{\mathbf{p}}$ yields the atomic virial theorem and the definition of

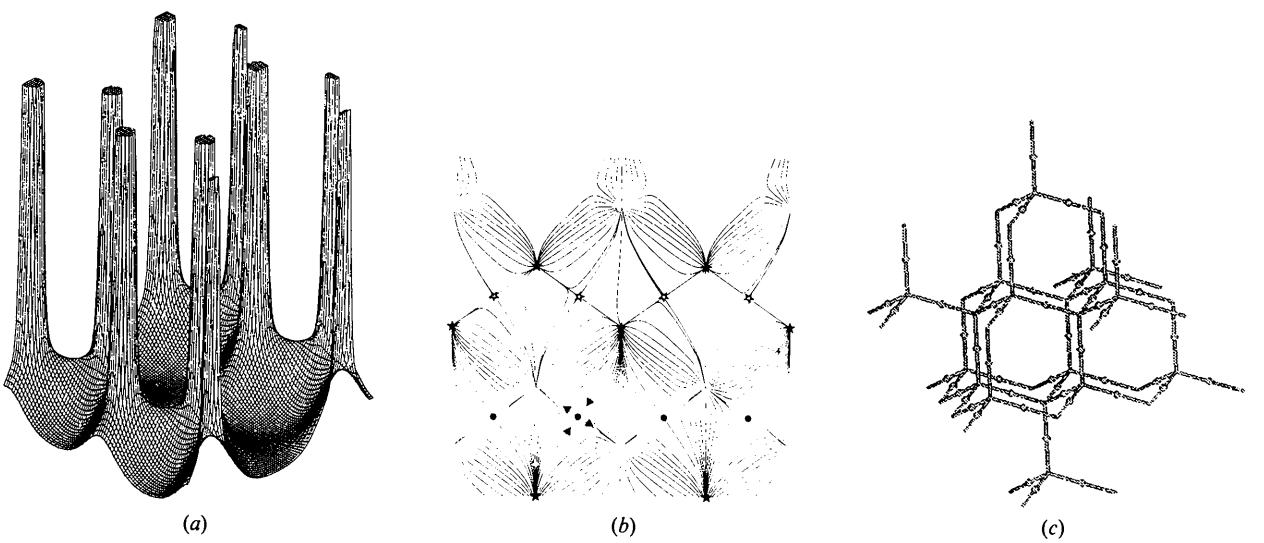

(*a*) (*b*) (*c*)

Fig. 1. (*a*) Relief map of the electronic charge distribution in a (110) plane of diamond. The charge density ρ exhibits local maxima only at the positions of the nuclei that behave as (3, −3) critical points. (*b*) Display of the trajectories traced out by the gradient vectors of ρ. The region of space traversed by trajectories terminating at a given nucleus, indicated by an open circle, is the atomic basin and an atom is the union of the nucleus and its basin. The saddles shown for ρ that link the nuclei in the foreground of (*a*) are critical points with one positive and two negative curvatures, (3, −1) or bond critical points, denoted by dots in (*b*). Arrows are shown for the pair of trajectories that terminate at one such bond critical point and define the intersection of an interatomic surface with this plane and for the pair that originate there and define the bond path. The trajectories terminating at a nucleus originate at (3, +3) or cage critical points, local minima in ρ (denoted by a full star), at (3, +1) or ring critical points (denoted by an open star) and one from each bond critical point (denoted by a dot). The central cage critical point of the $\nabla\rho$ map is visible in the relief map of ρ. The pair of trajectories originating at a bond critical point define the bond path – the line of maximum charge density linking neighbouring nuclei. Each C nucleus is linked by bond paths to four other C nuclei, two in the (110) plane and one above and the other below this plane to yield a tetrahedral structure. The resulting structure defined by the bond paths is indicated in (*c*). The saddles in ρ that link the nuclei in the foreground with those at the back are ring critical points and not bond critical points, both of which in this plane appear as (2,0) critical points.

the energy of the open system. Table 1 provides a summary of atomic theorems for generators that are fundamental in establishing the mechanics of an atom as a proper open quantum system (Bader & Popelier, 1993). The zero-flux surface of an atom Ω is denoted $S(\mathbf{r})$, the vector current density $\mathbf{J}(\mathbf{r})$, the quantum stress tensor $\sigma(\mathbf{r})$ and the electronic kinetic energy of the atom $T(\Omega)$. The divergence of a current density that appears in the local equations of motion obtained from Schrödinger's equation of motion for an observable $\hat{G}$ appears as the flux in the same current density through the surface of the atom. This agreement in form and content of the local and open-system equations of motion obtains only for a proper open system (Bader, 1994).

Since the zero-flux boundary condition stated in (1), when applied to an atom in a crystal, represents a generalization of the concept embodied in the original definition of a Wigner–Seitz cell, it is proposed that this name be applied to the proper systems found in solids. This identification of a Wigner–Seitz cell with a physical property of the system obviates a difficulty associated with the original construction of the polyhedral cell in that it does not lead to a physically unique decomposition in cases where more than one atom is associated with a lattice point.

This point is illustrated by the shape of the C atom defined by the four interatomic surfaces comprising its zero-flux surface in the face-centred-cubic diamond structure, which contains two atoms per unit cell (Fig. 2). Although it is possible to use the same recipe of bisecting the distances to the nearest-neighbour lattice points, 12 for a face-centred-cubic lattice, with perpendicular planes for the construction of a Wigner–Seitz cell (Slater, 1965), this construction does not reflect the basic form and symmetry of the charge distribution at the atomic level. Each of the four interatomic surfaces that separates the basin of a given C atom of $\mathscr{T}_d$ symmetry from its four bonded neighbours is seen to be curved with the form of a chaise-longue, as are the six such surfaces bounding the linked pair of atoms that constitute the unit cell, where a *primitive unit cell*, a *topological Wigner–Seitz cell*, is defined as *the smallest connected set of atomic basins that preserves the translational invariance of the lattice.*

As a consequence of this definition, each atom exhibits the basic local (or site) symmetry of the crystal as determined by its distribution of charge, while the symmetry of the cell reflects the translational invariance of the group of atoms that comprises the cell. For example, while the space group of diamond is O_h^7, each C atom is of $\mathscr{T}_d$ symmetry and the topological Wigner–Seitz cell is of $\mathscr{D}_{3d}$ symmetry (Fig. 2). Thus, while the topological definition given here will always reflect the physical symmetry imposed on the cell by the distribution of charge throughout the crystal, it will not, in the general case, preserve the full point-group symmetry of the lattice. Some may regard the preservation of this latter symmetry to be one of the most important features of the conventional definition, and here we acknowledge the view of a referee that use of the name Wigner–Seitz should be so restricted.

Table 1. *Atomic theorems for molecules and crystals*

Atomic force theorem $\hat{G} = \hat{\mathbf{p}}$

$$m\int_\Omega \mathrm{d}\mathbf{r}\,\partial\mathbf{J}(\mathbf{r})/\partial t = \int_\Omega \mathrm{d}\mathbf{r}\int \mathrm{d}\tau'\,\Psi^*(-\nabla\hat{V})\Psi + \oint \mathrm{d}S(\mathbf{r})\sigma(\mathbf{r})\cdot\mathbf{n}(\mathbf{r})$$

Atomic virial theorem $\hat{G} = \hat{\mathbf{r}}\cdot\hat{\mathbf{p}}$

$$m\int_\Omega \mathrm{d}\mathbf{r}\,\mathbf{r}\cdot\partial\mathbf{J}(\mathbf{r})/\partial t = 2T(\Omega) + \int_\Omega \mathrm{d}\mathbf{r}\int \mathrm{d}\tau'\,\Psi^*(-\mathbf{r}\cdot\nabla\hat{V})\Psi + \oint \mathrm{d}S(\mathbf{r})\mathbf{r}\cdot\sigma(\mathbf{r})\cdot\mathbf{n}(\mathbf{r})$$

Atomic torque theorem $\hat{G} = \hat{\mathbf{r}}\times\hat{\mathbf{p}}$

$$m\int_\Omega \mathrm{d}\mathbf{r}\,\mathbf{r}\times\partial\mathbf{J}(\mathbf{r})/\partial t = \int_\Omega \mathrm{d}\mathbf{r}\int \mathrm{d}\tau'\,\Psi^*(-\mathbf{r}\times\nabla\hat{V})\Psi - \oint \mathrm{d}S\sigma(\mathbf{r})\times\mathbf{r}\cdot\mathbf{n}$$

Atomic current theorem $\hat{G} = \hat{\mathbf{r}}$

$$\int_\Omega \mathrm{d}\mathbf{r}\,\mathbf{r}\,\partial\rho(\mathbf{r})/\partial t = \int_\Omega \mathrm{d}\mathbf{r}\,\mathbf{J}(\mathbf{r}) - \oint \mathrm{d}S\mathbf{J}(\mathbf{r})\mathbf{r}\cdot\mathbf{n}(\mathbf{r})$$

Atomic continuity theorem $\hat{G} = \hat{N}$

$$\int_\Omega \mathrm{d}\mathbf{r}\,\partial\rho(\mathbf{r})/\partial t = -\oint \mathrm{d}S\mathbf{J}(\mathbf{r})\cdot\mathbf{n}(\mathbf{r})$$

Atomic power theorem $\hat{G} = \hat{\mathbf{p}}^2/2m$, written without $1/2m$

$$\int_\Omega \mathrm{d}\mathbf{r}\,\partial\rho_{p^2}(\mathbf{r})/\partial t = \int_\Omega \mathrm{d}\mathbf{r}\int \mathrm{d}\tau'(\hbar/i)[(\Psi\nabla\Psi^* - \Psi^*\nabla\Psi)\cdot\nabla\hat{V}] + \oint \mathrm{d}S\mathrm{Re}[\mathbf{J}_{p^2}(\mathbf{r})]$$

$$\sigma(\mathbf{r}) = (\hbar^2/4m)\int \mathrm{d}\tau'[\nabla\nabla\Psi^*)\Psi - \nabla\Psi^*\nabla\Psi - \nabla\Psi\nabla\Psi^* + \Psi^*\nabla\nabla\Psi]$$

$$\mathbf{J}(\mathbf{r}) = (\hbar/2mi)\int \mathrm{d}\tau'(\Psi^*\nabla\Psi - \Psi\nabla\Psi^*)$$

Starting from the original definition of Wigner & Seitz for sodium metal, one can follow two paths to obtain a representation of the smallest space-filling volume for a crystal in the general case. One can apply the same geometrical method of construction starting from any lattice point, thereby preserving the lattice symmetry, the abstract symmetry of the crystal, but possibly losing its physical symmetry in real space. (The geometrical construction is the way to obtain the first Brillouin zone in reciprocal space.) Or, one can follow directly in the path of Wigner & Seitz and define the cell by generalizing the boundary condition that they imposed in an *ad hoc* manner to obtain a quantum description of an Na atom in the real space of a crystal. It was the pursuit of physics by Wigner & Seitz that led them to a definition of a cell that has since been shown to coincide with the general solution to this problem in the many-electron case, using a variational principle of physics. The proposal to apply the name Wigner–Seitz cell to the topogical cell satisfying the boundary condition in the general case follows the same philosopy: to extend the usefulness of the definition by endowing the cell with the physical reality that accompanies its quantum description.

This usefulness is exemplified by the observation that the properties of the proper open systems, as well as being additive to yield the corresponding

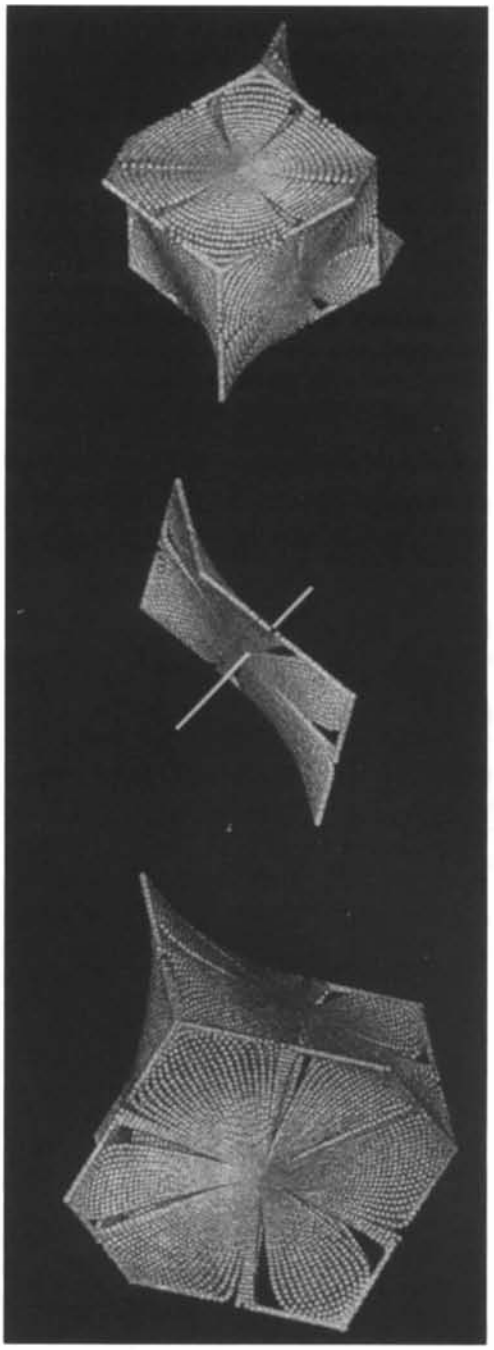

Fig. 2. Top: the region of space bounded by the four interatomic surfaces of zero flux in $\nabla\rho$ that define a C atom in diamond of $\mathscr{T}_d$ symmetry. Middle: an interatomic surface in diamond defined by the trajectories of $\nabla\rho$ terminating at the bond critical point, the point of maximum density at the centre of the surface. Also shown is the bond path defined by the unique pair of trajectories that originate at the critical point. There is a cage critical point at each of the six vertices of the surface with a ring critical point lying midway along each edge. Each vertex is shared by ten atoms, each edge by six. Bottom: a bonded pair of C atoms defining the Wigner–Seitz cell of diamond of $\mathscr{D}_{3d}$ symmetry, drawn to smaller scale. The threefold axis is directed out of the page through the central vertex.

values for the total system, are found to be transferable between molecules and in these instances have been shown to recover the measured properties of atoms in molecules (Bader, 1990). These include the energy and properties that measure the response of a system to externally applied fields, the electric polarizability (Bader, Gough, Laidig & Keith, 1992) and the magnetic susceptibility (Bader & Keith, 1993). It is this demonstrated agreement between measured and predicted properties that justifies the identification of the proper open systems with the chemical atom. The proper open systems are the most transferable pieces of system that can be defined in an exhaustive partitioning of real space and all the properties of a proper open system are found to be transferable to the same degree as its distribution of electronic charge. Thus, structure factors determined for a proper Wigner–Seitz cell in one crystal, or calculated for a fragment in a molecule, can be used in a structure determination of a crystal containing the cell or group in question. The use of a structure factor obtained for an atom in a molecule to describe the scattering by the same atom in a crystal is illustrated in this paper.

3. Structure in crystals

The word *connected* appearing in the definition of a unit cell is used in the usual sense to imply that the atoms comprising the cell are bonded to one another (Bader, Nguyen-Dang & Tal, 1981; Bader, 1990). A zero-flux surface shared by the basins of neighbouring atoms contains a critical point in ρ, a point $\mathbf{r}_c$ where $\nabla\rho(\mathbf{r}_c) = 0$, at which one of the three curvatures of ρ is positive, the other two being negative; a $(3,-1)$ or bond critical point. The set of trajectories of $\nabla\rho$ that terminate at the critical point at $\mathbf{r}_c$ defines the interatomic surface (Fig. 2). A unique pair of trajectories originates at each bond critical point, with each trajectory of the pair terminating at a nucleus of a neighbouring atom. They define a line linking the nuclei of the two atoms sharing a common surface along which the charge density is a maximum with respect to any neighbouring line (Figs. 1 and 2). Such a line when present in an equilibrium geometry is called a bond path and its presence fulfils the necessary and sufficient conditions that two atoms so linked be bonded to one another. The network of bond paths so generated, the molecular structure, has been shown to recover the bonded structures of molecules (Runtz, Bader & Messer, 1977; Bader, 1990). In the diamond structure, each carbon nucleus is linked to four neighbouring nuclei by bond paths, as anticipated by Bragg (1921) and illustrated in Fig. 1(*c*). The application of the definition of structure in terms of a network of bond paths requires knowledge of the

electron density. The bond-valence model of Brown (1977, 1992), which is widely used to assign a chemical structure to inorganic solids, on the other hand, has a purely empirical basis couched in terms of atomic and bond valences. A comparison of the structures obtained using the two approaches should better our understanding of the bond concept.

The trajectories that terminate at a $(3,-1)$ or bond critical point and define an interatomic surface orginate at local minima in the electron density that are $(3,+3)$ or cage critical (c) points and at $(3,+1)$ or ring critical (r) points, the electron density being a minimum in a ring surface. These two critical points, together with the bond critical (b) points and the local maxima at the positions of the nuclei (n), pseudo-$(3,-3)$ critical points, represent the four possible critical points of rank three (Collard & Hall, 1977). The topology of the electron density and its change with nuclear displacements, as reflected in the dynamics of its associated gradient vector field, yield a theory of molecular structure and structural stability (Bader, Nguyen-Dang & Tal, 1979, 1981). The use of critical points in the analysis of the electron density, without their identification with elements of structure, was described by Smith, Price & Absar (1977) and, for the case of crystals, Johnson (1977). Early analyses of experimental charge densities obtained from X-ray analysis using the theory of molecular structure were given by Lau, Bader, Hermansson & Berkovitch-Yellin (1986), Lobanov, Tsirelson & Belokonava (1988) and Kappkhan, Tsirelson & Ozerov (1989). Recent applications are described by Jeffrey & Piniella (1991) and by Destro, Bianchi, Gatti & Merati (1991).

One easily shows (Zou, 1993) that the Poincaré–Hopf relation governing the type and number of critical points for an extended system is given by

$$n - b + r - c = 0, \qquad (3)$$

a result first given by Johnson (1977). The critical points in the calculated densities for diamond and the homeomorphic zincblende structures AB serve as examples of the application of (3). There are two nuclei in each Wigner–Seitz cell and each is linked by four bond paths to its neighbours, one between the nuclei in the cell and six to neighbouring atoms, yielding $n = 2$ and $b = (1 + 6/2) = 4$. Each pair of bond paths terminating at a nucleus contributes to two six-membered rings and one atom therefore participates in 12 rings, yielding 24/6 or four rings per cell and $r = 4$. Each nucleus participates in two ways in ten-atom cage structures: in one, two of its bond paths contribute, in the other, three do. There is a total of six cages of the first kind and four of the second for a given nucleus and therefore one atom participates in ten cages to yield $c = 2(6/10 + 4/10) = 2$ cages per cell. This set of values for the structural parameters satisfies (3). There is only one type of ring in the zincblende structures AB but two types of ten-membered cage corresponding to $(4A,6B)$ and $(6A,4B)$. All cages in both types of structure are of $\mathcal{S}_d$ symmetry.

Table 2. *Values of bond, ring and cage critical points for crystals in atomic units and their correlation with bulk properties*

One atomic unit of density = 6.748 e Å^{-3} and of $\nabla^2\rho$ = 24.10 e Å^{-5}.

Crystal	C	BN	BP	Si	AlP
ρ_b	0.263	0.152	0.130	0.092	0.056
ρ_r ($\times 10^2$)	2.060	1.793	0.947	0.434	0.449
ρ_{c1} ($\times 10^2$)	1.281	1.153	0.600	0.237	0.247
ρ_{c2} ($\times 10^2$)		0.898	0.501		0.235
$\nabla^2\rho_c$ ($\times 10^2$)	7.493	7.445	2.363	0.915	0.905
E (Hartrees)*	0.555	0.498	0.383	0.345	0.317
ω (THz)	39.9[a]	31.62[a]	23.9[b]	15.53[a]	13.17[a]
B (GPa)	443[c]	367[b]	173[b]	99[c]	86[d]

References: (*a*) Weyrich, Brey & Christensen (1988); (*b*) Wentzcovitch, Chang & Cohen (1986); (*c*) Chang & Cohen (19850; (*d*) Zhang & Cohen (19850.

* All values from Orlando, Dovesi, Roetti & Saunders (1990) and corrected for zero-point energies. 1 Hartree = 1 a.u. of energy.

International Tables for Crystallography (Hahn, 1983) can be used as an aid in locating all of the critical points in a crystal, a point first made by Johnson (1977). The site symmetries contained therein correlate with the symmetries of the critical points that determine the structural elements. In diamond, for example, according to the table for the space group $Fd3m$ (O_h^7, No. 227), two nuclei in a primitive cell are located at the position labelled a, four bond critical points at position c, four ring critical points at d and two cage critical points at b. For the zincblende structures, one uses the table for $F\bar{4}3m$ (T_d^2, No. 216). The A and B nuclei are located at the a and c positions, respectively, bond and ring critical points at positions e, with different values for the parameter x, the cages $(4A,6B)$ at positions b and $(6A,4B)$ cages at d.

Table 2 lists the properties of the density at the critical points in the diamond and zincblende structures; ρ_b is the value of $\rho(\mathbf{r})$ at the bond critical point, ρ_r the value at the ring critical point and ρ_c and $\nabla^2\rho_c$ the corresponding values at the cage critical points, the latter values averaged over the two kinds of cage critical points in the AB structures. The net charges on the atoms in the AB structures, as determined by an integration of ρ over the basin of the atom and its subtraction from the nuclear charge, are ± 2.4 e for both BN and AlP, and ± 1.6 e for BP. The populations indicate that the relative electronegativities of the group III and V elements from the second row are the same as for their third-row congeners, while the third-row element P is only two-thirds as electronegative as the second-row element N from the same family.

Eberhart, Donovan, MacLaren & Clougherty (1991) have used the theory of structure to relate the bulk mechanical properties of metals and alloys to the properties of $\rho(\mathbf{r})$ at its critical points. To illustrate the existence of similar relationships in the diamond and zincblende structures, Table 2 includes values of their binding energies E, transverse optical frequencies ω and bulk moduli B. The value of the density at a bond critical point, ρ_b, provides a measure of bond order and bond strength in molecules and is found to provide a similar measure in solids. The bulk properties E, ω and B exhibit the same trend in values as ρ_b, decreasing from a maximum in diamond to a minimum in AlP. The quantity ω is the frequency associated with a bond stretch and is expected to correlate directly with ρ_b. The bulk modulus $B = (\Delta P/\Delta V)/V$ or modulus of volume elasticity has the dimensions of pressure or energy density. The Laplacian of ρ, the sum of the three curvatures of ρ, occurs throughout the theory multiplied by $\hbar^2/4m$ and the quantity $(\hbar^2/4m)\nabla^2\rho$ has the dimensions of energy density, the same as B. Eberhart, Donovan, MacLaren & Clougherty (1991) have related the bulk modulus of close-packed metals to the curvature of ρ_b parallel to the bond path. Relative to the body-centred-cubic (b.c.c.) metals, the diamond and zincblende structures are relatively open, with the density attaining its minimum values at the cage critical points. Compressing the crystal changes the volume of the cages and the larger the curvature of the density at the cage critical point, the more resistant is the crystal to a compression, the values of $\nabla^2\rho_c$ exhibiting the same trend as those of B.

Using the structural relationship in (3), one finds that an atom at the b.c.c. lattice point can be linked by bond paths to its six next-nearest neighbours, as well as to its eight nearest neighbours. In this structure, an atom is bounded by 14 interatomic surfaces, in agreement with the original definition of a Wigner–Seitz cell for a b.c.c. lattice. Eberhart, Donovan, MacLaren & Clougherty (1991) find this pattern of bond paths, that is, this *structure*, to be predicted by the calculated charge distributions of b.c.c. transition metals and have also demonstrated the absence of bond paths to second-nearest neighbours in metals possessing the face-centred-cubic (f.c.c) lattice, a result again in agreement with (3). The topological analysis has been applied by Eberhart, Clougherty & MacLaren (1993) to the differing ductility of intermetallic alloys CuAu and TiAl and by Eberhart, Donovan & Outlaw (1992) to the diffusivity of O atoms in group I*B* transition metals. Mei, Edgecombe, Smith & Heilingbrunner (1993) have analysed the topology of the theoretical charge densities and the structures they predict for the b.c.c. lattices of lithium and sodium, results that are discussed in more detail below.

4. Atomic basis of the elastic X-ray scattering from crystals

If one keeps only the first-order terms in the perturbative development of the interaction between X-rays and the electrons of a crystal, the measurable differential cross section of the elastically scattered X-rays can be expressed in terms of the scattering caused by a single free electron, the Thomson-scattering cross section T_0, modified by the square of a term $\mathcal{F}(\mathbf{k} - \mathbf{k}')$ representing the Fourier transform of the electron-density distribution of the crystal:

$$d\sigma/d\Omega = T_0|\mathcal{F}(\mathbf{k} - \mathbf{k}')|^2. \quad (4)$$

The Fourier transform or scattering amplitude is

$$\mathcal{F}(\mathbf{k} - \mathbf{k}') = \int d\mathbf{r}\rho(\mathbf{r}) \exp i(\mathbf{k} - \mathbf{k}') \cdot \mathbf{r}, \quad (5)$$

where the wave vectors of the incident and elastically scattered X-rays are related by $|\mathbf{k}| = |\mathbf{k}'|$. The scattering amplitude can be equated to the amplitude of the scattering from one cell in the crystal, repeated over each lattice point. The Laue condition for diffraction is met when $\Delta\mathbf{k}/2\pi = (\mathbf{k} - \mathbf{k}')/2\pi$ equals a reciprocal-lattice vector $\mathbf{G}$ of the crystal, where $\mathbf{G} = h\mathbf{A} + k\mathbf{B} + l\mathbf{C}$. In this case, the scattering amplitude from a single unit cell expressed in terms of the fractional coordinates x, y and z is given by

$$F(\mathbf{G}) \equiv F(hkl) = \int_{\Omega_o} d\mathbf{r}\rho(\mathbf{r}) \exp 2\pi i(hx + ky + lz), \quad (6)$$

which is the so-called structure factor. The cell denoted by Ω_o is taken to be the primitive cell composed of the smallest set of connected atomic basins satisfying the condition of translational invariance, a topological Wigner–Seitz cell. This construction maximizes the relation of the cell to the physical form and symmetry exhibited by the charge distribution of the atoms making up the crystal, as illustrated in Fig. 2 for the diamond crystal. Any function invariant under a lattice translation can be expanded in a Fourier series and, in particular, the charge distribution of a crystal can be expressed as

$$\rho(\mathbf{r}) = V^{-1} \sum_{hkl} F(hkl) \exp 2\pi i\mathbf{G} \cdot \mathbf{r}, \quad (7)$$

where V is the volume of a unit cell.

The scattering amplitude for a crystal of N cells is thus determined by N times the structure factor for a single cell. The structure factor in turn is given by a sum of contributions from each atom j in the cell Ω_o. This contribution, called the atomic form factor $f(j,\mathbf{G})$, is determined by an integration of the appropriate density over the basin of the atom,

$$f(j,\mathbf{G}) = \int_j d\mathbf{r}\rho(\mathbf{r}_j) \exp 2\pi i\mathbf{G} \cdot \mathbf{r}_j, \quad (8)$$

where the coordinate $\mathbf{r}_j = \mathbf{r} - \mathbf{R}_j$ is referenced to the nucleus of atom j with position coordinate $\mathbf{R}_j$. An atomic form factor is the integral of the electron

density over the atom, weighted by the phase factor appropriate for a given reflection. For $h = k = l = 0$, that atomic form factor equals the average electron population of the atom in the crystal

$$f(j,\mathbf{0}) = N(j) = \int_j \mathrm{d}\mathbf{r}\rho(\mathbf{r}_j). \tag{9}$$

The structure factor, expressed in terms of the atomic form factors, is

$$F(\mathbf{G}) = \sum_j f(j,\mathbf{G}) \exp 2\pi i \mathbf{G}\cdot\mathbf{R}_j. \tag{10}$$

This expression for the structure factor is formally the same as that used in the conventional treatments, wherein the charge distribution over the unit cell is expressed as a superposition of atomic contributions, contributions that overlap one another within the cell and extend over into neighbouring cells. The expression given in (10) preserves the number of electrons within the cell by using nonoverlapping atomic contributions. The form of (10) is a consequence of the topology of the charge density partitioning a crystal into a set of quantum open systems.

5. Atomic scattering factors in diamond and silicon

The integers of the reciprocal-lattice vector $\mathbf{G}(hkl)$ must be all even or all odd for a reflection to occur in the f.c.c. lattice of diamond or silicon. The reflections fall into three classes; those with $h + k + l = 4n$, $4n \pm 1$ and $4n + 2$ (Kittel, 1986). The primitive unit cell contains two atoms with nuclear coordinates $(-\frac{1}{8},-\frac{1}{8},-\frac{1}{8})$ and $(\frac{1}{8},\frac{1}{8},\frac{1}{8})$ with the origin taken at the inversion centre. Equation (10) gives the scattering amplitude of a Wigner–Seitz unit cell to be

$$\begin{aligned} F(\mathbf{G}) &= \int_1 \rho(\mathbf{r}_1) \exp(2\pi i \mathbf{G}\cdot\mathbf{r}_1)\mathrm{d}\mathbf{r}_1 \\ &\quad + \int_2 \rho(\mathbf{r}_2) \exp(2\pi i \mathbf{G}\cdot\mathbf{r}_2)\mathrm{d}\mathbf{r}_2. \end{aligned} \tag{11}$$

Atom 2 is related to atom 1 by translation $(\frac{1}{4},\frac{1}{4},\frac{1}{4})$ followed by an inversion at nucleus 2. The atomic form factor of atom 1 can alternatively be expressed as $f_1 = A + iB$. The inversion relation between atoms 1 and 2 then yields $f_2 = A - iB$ and the total scattering power from the primitive unit cell can be written as

$$\begin{aligned} F(\mathbf{G}) &= \exp[-\pi i(h + k + l)/4](A + iB) \\ &\quad + \exp[\pi i(h + k + l)/4](A - iB) \\ &= 2A\cos[\pi(h + k + l)/4] \\ &\quad + 2B\sin[\pi(h + k + l)/4]. \end{aligned} \tag{12}$$

The 'forbidden' 222 reflection belongs to the $4n + 2$ set for which (12) gives

$$F(4n + 2) = 2(-1)^n B. \tag{13}$$

The quantity B, which determines the noncentrosymmetric component of the atomic charge density, can be written as

$$B = \int_0^{2\pi} \mathrm{d}\varphi \int_0^{\pi} \sin\theta \mathrm{d}\theta \oint \mathrm{d}S(\mathbf{r}_s)\rho(\mathbf{r}_1) \sin(2\pi\mathbf{G}\cdot\mathbf{r}_1) r_1^2 \mathrm{d}r_1, \tag{14}$$

where the radial integral is from the origin to the value of r_1 on the surface of the atom, and where A, the centrosymmetric part, is given by the corresponding cosine function. Because of the $\mathcal{S}_d$ symmetry of the atom, A or B can be evaluated over a reduced region of the atomic basin, B for example being

$$\begin{aligned} B = \int_0^{\pi} \mathrm{d}\varphi \int_0^{\pi/2} &\sin\theta \mathrm{d}\theta \oint \mathrm{d}S(\mathbf{r}_s)\rho(\mathbf{r}_1) \\ &\times [\sin 2\pi(hx + ky + lz) + \sin 2\pi(hx - ky - lz) \\ &+ \sin 2\pi(-hx + ky - lz) \\ &+ \sin 2\pi(-hx - ky + lz)] r_1^2 \mathrm{d}r_1. \end{aligned} \tag{15}$$

The C and Si atoms in the crystal, unlike their spherical-atom counterparts, have no inversion symmetry and B does not necessarily vanish. However, the value of B is determined entirely by the departure of the atom's charge distribution from spherical symmetry and in general $4n + 2$ reflections are weak and some, like 200, are totally absent. This is a result of the interference occurring within the basin of an individual atom, as happens whenever at least one of h, k or l is zero.

With the program *CRYSTAL* and the basis set described above, the value of $F(222)$ for a vibrationless diamond crystal, the static structure factor, with the lattice constant set equal to the experimental value of 3.5667 Å, is calculated to be 1.207 e for the eight C atoms in the conventional unit cell, the unit used throughout this section. This agrees with the static value of 1.208 (80) e (Aleksandrov, Tsirelson, Reznik & Ozerov, 1989) obtained from the experimental scattering factor (Göttlicher & Wölfel, 1959). The R factor, which provides a measure of the overall agrement between the calculated and the nine experimentally measured structure factors for diamond, is found to be 0.023.

The basin of the central C atom in *neo*-pentane is totally enclosed by the interatomic surfaces shared with four tetrahedrally linked C atoms and it can serve as a model of the atom in diamond. The charge distribution for this atom can be determined in a calculation using a relatively large basis set, in which the C–C bond lengths in the molecule are fixed at the value of 1.5445 Å found in the crystal. The value of $F(222)$ is calculated to be 1.064. The C atom in this case has an average population of 5.817 e, as determined by the integration of $\rho(\mathbf{r})$ over its basin, and the value of $F(222)$ normalized to six electrons is

increased to 1.087. The phase angles for diamond are either zero or π depending upon choice of origin. The phase for the 222 reflection is predicted to be zero using the crystal or the molecular C atom, a result in agreement with the phase obtained in the refinement of the experimental data. Atoms in a given valence state and their properties are frequently transferable to the extent found here for carbon. Even the shape of the C–C interatomic surface in diamond (Fig. 2) is the same as that found in *neo*-pentane or ethane. The R factor for diamond using the atomic form factors obtained for the central carbon in neopentane is 0.023, the same as that obtained by a direct calculation for the crystal, using a smaller basis set.

Both experiment (Sakata & Sato, 1990) and theory (Orlando, Dovesi, Roetti & Saunders, 1990) show the charge distribution of crystalline silicon to be exceptional in that the charge density exhibits local maxima located midway between the nuclei. Such maxima behave as non-nuclear attractors in the gradient vector field of $\rho(r)$ and give rise to pseudo-atoms in the crystal (Fig. 3). Pseudo-atoms were first found in clusters of group I metal atoms (Gatti, Fantucci & Pacchioni, 1987; Cao, Gatti, MacDougall & Bader, 1987). The charge density at the local maximum in a pseudo-atom exceeds that at the neighbouring bond critical points that link it to the neighbouring atoms by only small amounts. Thus, the charge density in the central region between nuclei linked by bond paths to a pseudo-atom is relatively flat with $\rho(\mathbf{r})$ exhibiting only small curvatures, compared with those exhibited by $\rho(\mathbf{r})$ at the critical point of the bond path linking two nuclei directly. Table 3 compares the values of $\rho(\mathbf{r})$ and its curvatures, λ_i, at the non-nuclear attractor in silicon with those at the bond critical points of diamond and silicon. The small curvatures associated with the charge maximum of a non-nuclear attractor imply that the density has a low kinetic energy per electron (Cao, Gatti, MacDougall & Bader, 1987) and that it is therefore loosely bound. This follows from the local statement of the virial theorem (Bader, 1990)

$$(\hbar^2/4m)\nabla^2\rho(\mathbf{r}) = 2G(\mathbf{r}) + \mathcal{V}(\mathbf{r}), \qquad (16)$$

where $G(\mathbf{r})$ is the kinetic energy density, defined as $(1/2m)\int d\tau'(\hat{\mathbf{p}}\psi)^* \cdot \hat{\mathbf{p}}\psi > 0$, and $\mathcal{V}(\mathbf{r}) < 0$ is the potential energy density, the virial of the local Ehrenfest force exerted on the electrons. Silicon possesses pseudo-atoms and is a semiconductor. Diamond, with the same lattice structure but with no pseudo-atoms, is an insulator. The value of $\nabla^2\rho(\mathbf{r})$ at a bond critical point in diamond, compared with the corresponding value for silicon (Table 3), from (16) demonstrates the much tighter binding of the valence charge density in diamond compared with that in silicon.

This analysis of the electron density in the clusters of lithium and sodium suggests a model of group I metals wherein the positively charged atoms with localized charge distributions are bound by an intermeshed network of negatively charged pseudo-atoms, whose loosely bound and delocalized electronic charge is responsible for the binding and the conducting properties of the metals.

The calculated electron densities for the b.c.c. lattices of lithium and sodium obtained by Mei, Edgecombe, Smith & Heilingbrunner (1993) using the program *CRYSTAL* do indeed predict the presence of pseudo-atoms in both crystals. In b.c.c. lithium, the pseudo-atoms are connected by bond paths as in the metallic clusters, but not in b.c.c. sodium. What is important for the understanding of the properties of the systems in which pseudo-atoms are found is not so much their presence, as the finding that the distribution of electronic charge in the interatomic valence region is diffuse, loosely bound and nearly devoid of curvature.

An Si atom and a pseudo-atom for the crystal are displayed in Fig. 4. The interatomic surfaces for an Si atom, like those for a C atom in diamond, are curved in the form of a chaise-longue, but in this case the surfaces are concave since a pseudo-atom, with a finite volume and an average electron population of 0.958, links every pair of neighbouring Si atoms. Unlike an atom of diamond, a pseudo-atom exhibits $\mathcal{D}_{3d}$ symmetry and possesses a centre of symmetry. Structure factors were calculated for the experimental value of the lattice constant of 5.431 Å. The contribution to $F(222)$ from the eight

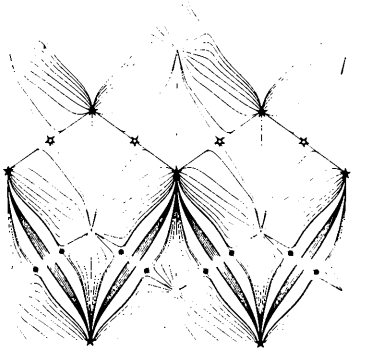

Fig. 3. A display of the trajectories of $\nabla\rho$ for the silicon crystal in the (110) plane. The Si atoms are not bonded directly to one another as are the C atoms in diamond (*cf.* Fig. 2) but rather through intervening pseudo-atoms whose basins are defined by the trajectories of $\nabla\rho$ terminating at the $(3,-3)$ critical point located midway between the Si nuclei. A pseudo-atom has an average electron population of 0.96. The value of ρ at its maximum exceeds that at the neighbouring bond critical points by only 0.2213 a.u. Thus, the density of a pseudo-atom that links pairs of Si atoms is nearly devoid of curvature and is of relatively low value, features characteristic of loosely bound electron density.

Table 3. *Properties of electronic charge density $\rho(\mathbf{r})$ at critical points in diamond and silicon lattices in atomic units*

Subscripts b and n denote bond critical point and non-nuclear attractor, respectively, with curvatures $\lambda_1 = \lambda_2$ perpendicular to the bond axis.

Crystal	ρ_b	$\lambda_1 = \lambda_2$	λ_3	$\nabla^2\rho_b$	ρ_n	$\lambda_1 = \lambda_2$	λ_3	$\nabla^2\rho_n$
Diamond	0.2626	−0.500	0.199	−0.881				
Silicon	0.0922	−0.083	0.078	−0.088	0.0935	−0.085	−0.0002	−0.150

crystal Si atoms in the conventional unit cell is calculated using (9) and (10) to be −2.030. There are four non-nuclear attractors in a Wigner–Seitz cell of silicon, at (0,0,0), $(0,\frac{1}{4},\frac{1}{4})$, $(\frac{1}{4},0,\frac{1}{4})$ and $(\frac{1}{4},\frac{1}{4},0)$, and their contribution to the scattering amplitude is given by

$$F^n(hkl) = f_1^n + f_2^n \exp[i\pi(k+l)/2] + f_3^n \exp[i\pi(h+l)/2] + f_4^n \exp[i\pi(h+k)/2]. \quad (17)$$

Since the pseudo-atom has a centre of symmetry, the imaginary contribution to its form factor f_j^n is identically zero. Since the sum of any two indices $h + k$ is always even for a reflection in a diamond lattice, $(h + k)/2$ is an integer in (17) and thus the contribution from the pseudo-atoms to the structure factor is always real. The contribution to the 222 reflection from the 16 pseudo-atoms in the conventional cell is calculated to be 3.610. The calculated static structure factor for the 222 reflection is thus 1.580, compared with the static values of 1.526 (Lu & Zunger, 1992) and 1.544 (Spackman, 1986) obtained from experiment. Note that the charge distribution of a pseudo-atom determines the phase and dominates the value of the structure factor for the 222 reflection, their presence isolating the dominant tetrahedral component to the valence-charge distribution. The 222 structure factor calculated for an Si atom in the silicon analogue of neopentane with an atomic population of 14.0 is found to be 1.690.

Lu & Zunger (1992) obtained a value for $F(222)$ of 1.344 in an *ab initio* calculation using the local density formalism. Sakata & Sato (1990) have used the maximum-entropy method to determine the charge density of the silicon crystal using 30 accurately measured structure factors (Saka & Kato, 1986). The density so determined was then used to calculate the structure factors for the 'forbidden' reflections. This yielded a value of 1.527 for the 222 reflection at room temperature. In their analysis, the charge density exhibits a maximum midway between pairs of Si nuclei with $\rho(\mathbf{r}) = 0.10$ a.u. This agrees satisfactorily with the value of 0.09 a.u. calculated for the local density maximum at the position of the non-nuclear attractor (Table 3).

The calculated atomic and pseudo-atomic contributions to the static structure factors are given in Table 4 for silicon, along with the corresponding values obtained from experiment (Lu & Zunger, 1992; Spackman, 1986). The imaginary contribution from the atomic form factor, the B contribution, does or does not vanish depending on whether or not there is local interference over the basin of the atom. The value of $F(000)$ is a measure of the goodness of the numerical integration used to determine the atomic form factors. The percentage error in its

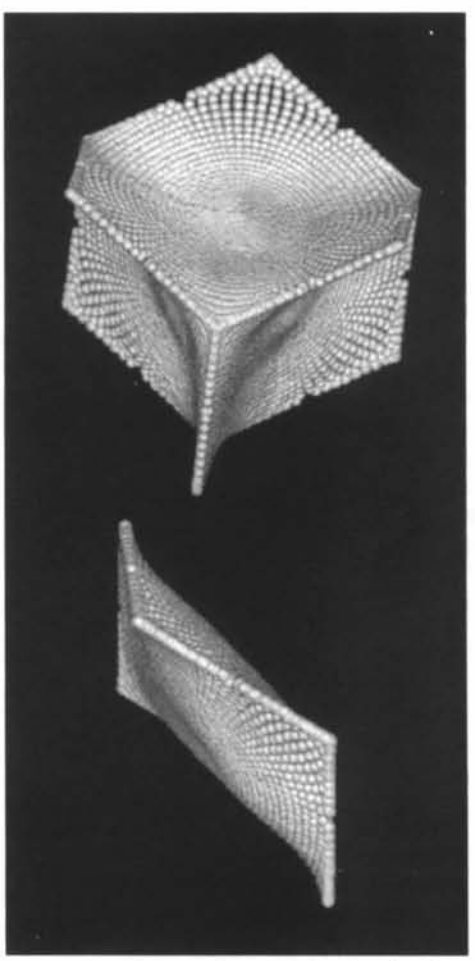

Fig.4. Top: region of space bounded by the four interatomic surfaces defining an atom in the silicon crystal. Its shape is homeomorphic with that for a C atom in diamond but the surfaces are concave since each is shared with a pseudo-atom (bottom). The pseudo-atom is of $\mathscr{D}_{3d}$ symmetry, with the threefold axis passing through the two bond critical points.

Table 4. *Calculated and experimental static structure factors and their atomic contributions for silicon*

$R = \sum|F_{cal} - F_{exp}|/\sum|F_{exp}| = 4.1 \times 10^{-3}$.

	Atomic contribution			$F(hkl)$	
(hkl)	A	B	F^n	Calculated	Experimental
(000)	12.0861	0.0000	15.3330	112.0218	
(111)	10.4274	−0.1865	−2.8756	−60.8068	−60.6873
(220)	8.8987	0.0000	2.2431	−68.9464	−69.2456
(311)	8.3023	−0.1304	2.5366	−45.1660	−45.3502
(222)	7.9404	−0.2537	3.6098	1.5802	1.5264
(400)	7.6333	0.0000	1.4450	−59.6191	−59.5944
(331)	7.1556	−0.0846	1.0690	41.0685	40.9969
(422)	6.6004	−0.0144	1.0259	53.8293	53.7296
(511)	6.4464	−0.0119	0.1096	36.5085	36.4194
(333)	6.2547	0.1263	1.6594	36.3266	36.3566
(440)	6.0651	0.0000	0.1435	48.6639	48.3696
(444)	5.0489	0.1441	0.5141	−39.8750	−39.8328
(551)	4.8013	−0.0153	−0.2202	−27.2940	−27.1936
(642)	4.5360	0.0272	−0.1594	−36.4471	−36.4384
(800)	4.1735	0.0000	0.1678	33.5555	33.4112
(660)	3.8865	0.0000	0.6174	−30.4748	−30.9304
(555)	3.8540	−0.0508	−0.2368	21.1641	21.2692
(844)	3.1530	−0.0189	−0.2973	24.9264	25.0800
(880)	2.5360	0.0000	0.4971	20.7848	20.2648

value is 0.02% of the correct value of $8 \times 14 = 112$. The total electron population calculated for an Si atom and two pseudo-atoms is 14.0027 e, in error by 0.0027 e.

5. Concluding remarks

The definition of a Wigner–Seitz cell in terms of the atoms in a crystal extends its usefulness and can increase our understanding of the properties of crystals. While only two atomic properties have been discussed here, atomic populations and form factors, the reader is reminded that every property of an atom in a crystal is defined, as illustrated in Table 1, and that each makes an additive contribution to the corresponding property of the total system. The zero-flux boundary condition enables one to go beyond the condition of translational invariance in the identification of the open systems that are physically important in the study of the solid state. One can, for example, define and differentiate between an adsorbed atom and the adsorbing surface of a solid, between an atom in the bulk of a solid and one in its surface layer and between a defect atom and its host. In every case, one obtains a complete description of all observable properties of the solid in terms of its atomic contributions. The ability to separately define the contributions of an interior and a surface atom to the total energy, for example, is of importance in the emerging field of nanostructures.

In addition to the above, the properties of the proper Wigner–Seitz cells reflect the transferability that is the operational characteristic of the atomic and functional-group model of matter. The charge distribution and hence the properties of a peptide group, for example, are transferable to a high degree from di- to polypeptides (Chang & Bader, 1992; Bader, Popelier & Chang, 1992; Popelier & Bader, 1994). These groups, defined by their two amidic interatomic surfaces as |NH–CHR–C(=O)|, bear a zero net charge. Their charge distributions, determined in calculations on model systems, can be used to predict the van der Waals shape, the electrostatic potential field and the structure factors of a polypeptide in terms of their atomic contributions. The method of atoms in crystals offers the opportunity of comparing directly the form and properties of an atom or group as it occurs in different systems.

We acknowledge the useful comments made by Professor V. G. Tsirelson of the Mendeleev Institute regarding this paper.

References

ALEKSANDROV, Y. V., TSIRELSON, V. G., REZNIK, I. M. & OZEROV, R. P. (1989). *Phys. Status Solidi*, **155**, 201–207.

BADER, R. F. W. (1990). *Atoms in Molecules – a Quantum Theory*. Oxford Univ. Press.

BADER, R. F. W. (1994). *Phys. Rev.* B**49**, 13348–13356.

BADER, R. F. W. & BEDDALL, P. M. (1972). *J. Chem. Phys.* **56**, 3320–3329.

BADER, R. F. W., GOUGH, K. M., LAIDIG, K. E. & KEITH, T. A. (1992). *Mol. Phys.* **75**, 1167 1189.

BADER, R. F. W. & KEITH, T. A. (1993). *J. Chem. Phys.* **99**, 3683–3693.

BADER, R. F. W. & NGUYEN-DANG, T. T. (1981). *Adv. Quantum Chem.* **14**, 63–124.

BADER, R. F. W., NGUYEN-DANG, T. T. & TAL, Y. (1979). *J. Chem. Phys*, **70**, 4316–4329.

BADER, R. F. W., NGUYEN-DANG, T. T. & TAL, Y. (1981). *Rep. Prog. Phys.* **44**, 893–948.

BADER, R. F. W. & POPELIER, P. A. L. (1993). *Int. J. Quantum Chem.* **45**, 189–207.

BADER, R. F. W., POPELIER, P. A. L. & CHANG, C. (1992). *J. Mol. Struct.* **255**, 145–171.

BIEGLER-KÖNIG, F. W., BADER, R. F. W. & TANG, T.-H. (1982). *J. Comput. Chem.* **13**, 317–328.

BINKLEY, J. S., POPLE, J. A. & HEHRE, W. J. (1980). *J. Am. Chem. Soc.* **102**, 939–947.

BRAGG, W. H. (1915). *Philos. Trans. R. Soc. London Ser. A*, **215**, 153.

BRAGG, W. H. (1921). *Proc. Phys. Soc. London*, **33**, 304–311.

BROWN, I. D. (1977). *Acta Cryst.* B**33**, 1305–1310.

BROWN, I. D. (1992). *Acta Cryst.* B**48**, 553–572.

CAO, W. L., GATTI, C., MACDOUGALL, P. J. & BADER, R. F. W. (1987). *Chem. Phys. Lett.* **141**, 380–385.

CHANG, C. & BADER, R. F. W. (1992). *J. Phys. Chem.* **96**, 1654–1662.

CHANG, K. J. & COHEN, M. L. (1987). *Phys. Rev. B*, **35**, 8196–8201.

COLLARD, K. & HALL, G. G. (1977). *Int. J. Quantum Chem.* **12**, 623–637.

DAWSON, B. (1967). *Proc. R. Soc. London Ser. A*, **298**, 255–288.

DESTRO, R., BIANCHI, R., GATTI, C. & MERATI, F. (1991). *Chem. Phys Let.* **186**, 47–52.

EBERHART, M. E., CLOUGHERTY, D. P. & MACLAREN, J. M. (1993). *J. Mater. Res.* **8**, 438–448.

EBERHART, M. E., DONOVAN, M. M., MACLAREN, J. M. & CLOUGHERTY, D. P. (1991). *Prog. Surf. Sci.* **36**, 1–34.

EBERHART, M. E., DONOVAN, M. M. & OUTLAW, R. A. (1992). *Phys. Rev. B*, **46**, 12744–12747.
GATTI, C., FANTUCCI, P. & PACCHIONI, G. (1987). *Theor. Chim. Acta*, **72**, 433–458.
GÖTTLICHER, S. & WÖLFEL, E. (1959). *Z. Electrochem.* **63**, 891–901.
HAHN, T. (1983). *International Tables for Crystallography*, Vol. A. Boston: Reidel. (Present distributor Kluwer Academic Publishers, Dordrecht.)
JEFFREY, G. A. & PINIELLA, J. F. (1991). Editors. *The Application of Charge-Density Research to Chemistry and Drug Design. NATO Adv. Study Inst. Ser. B*, No. 250.
JOHNSON, C. K. (1977). Am. Crystallogr. Assoc. Winter Meet., Asilomar. Abstracts, p. 30.
KAPPKHAN, M., TSIRELSON, V. G. & OZEROV, R. P. (1989). *Dokl. Phys. Chem.* **303**, 1025–1029.
KITTEL, C. (1986). *Introduction to Solid State Physics*. New York: Wiley.
LAU, C. D. H., BADER, R. F. W., HERMANSSON, K. & BERKOVITCH-YELLIN, Z. (1986). *Chem. Scr. Abstr.* **26**, 476.
LOBANOV, N. N., TSIRELSON, V. G. & BELOKONAVA, E. L. (1988). *Russ. J. Inorg. Chem.* **33**, 1740–1744.
LU, Z. W. & ZUNGER, A. (1992). *Acta Cryst.* A**48**, 545–554.
MEI, C., EDGECOMBE, K. E., SMITH, V. H. & HEILINGBRUNNER, A. (1993). *Int. J. Quantum Chem.* **48**, 287–293.
ORLANDO, R., DOVESI, R., ROETTI, C. & SAUNDERS, V. R. (1990). *J. Phys. Condens. Matter*, **2**, 7769–7789.
PISANI, C., DOVESI, R. & ORLANDO, R. (1992). *Int. J. Quantum Chem.* **42**, 5–33.
PISANI, C., DOVESI, R. & ROETTI, C. (1988). *Hartree–Fock Ab Initio Treatment of Crystalline Systems, Lecture Notes in Chemistry*, Vol. 48. Heidelberg: Springer-Verlag.
POPELIER, P. L. A. & BADER, R. F. W. (1994). *J. Phys. Chem.* **98**, 4473–4481.
RUNTZ, G. R., BADER, R. F. W. & MESSER, R. (1977). *Can. J. Chem.* **55**, 3040–3045.
SAKA, T. & KATO, N. (1986). *Acta Cryst.* A**42**, 469–478.
SAKATA, M. & SATO, M. (1990). *Acta Cryst.* A**46**, 263–270.
SCHWINGER, J. (1951). *Phys. Rev.* **82**, 914–927.
SLATER, J. C. (1934). *Phys. Rev.* **45**, 794–801.
SLATER, J. C. (1965). *Quantum Theory of Molecules and Solids*, pp. 14–23. New York: McGraw-Hill.
SMITH, V. H., PRICE, P. F. & ABSAR, I. (1977). *Isr. J. Chem.* **16**, 187–197.
SPACKMAN, M. A. (1986). *Acta Cryst.* A**42**, 271–281.
WENTZKOVITCH, R. M., CHANG, K. J. & COHEN, M. L. (1986). *Phys. Rev. B*, **34**, 1071–1079.
WEYRICH, K. H., BREY, L. & CHRISTENSEN, N. E. (1988). *Phys. Rev. B*, **38**, 1392–1396.
WIGNER, E. & SEITZ, F. (1933). *Phys. Rev.* **43**, 804–810.
ZHANG, S. B. & COHEN, M. L. (1987). *Phys. Rev. B* **35**, 7604–7610.
ZOU, P. F. (1993). PhD thesis, McMaster Univ., Hamilton, Ontario, Canada.

Acta Cryst. (1994). A**50**, 725–730

Study of Thermal Behaviour of Oxygen in Silicon Crystals by Analysis of X-ray *Pendellösung* Fringes

BY MING LI, ZHEN-HONG MAI AND SHU-FAN CUI

Institute of Physics, Chinese Academy of Sciences, PO Box 603, *Beijing* 100080, *People's Republic of China*

(*Received* 12 *October* 1993; *accepted* 21 *April* 1994)

Abstract

The thermal behaviour of oxygen in Czochralski (CZ) silicon and magnetic Czochralski (MCZ) silicon crystals was investigated by analysis of *Pendellösung* fringes based on the statistical theory of X-ray dynamical diffraction. The size and the density of oxygen precipitates were determined for different annealing temperatures and/or different times. It was observed that oxide precipitates in the samples increase in size and decrease in density with time during isothermal annealing at 1023 K. The precipitation in MCZ silicon approaches saturation level after annealing for 250 h. It was found that the size of precipitates increases rapidly with annealing temperature in isochronal annealing for 18 h. Comparison of the results of MCZ silicons with those of CZ silicons shows that MCZ crystals are thermally more stable. This suggests that magnetic fields can control the oxygen concentration effectively and that the MCZ and CZ silicon have different thermal behaviours. A powerful technique for detecting microdefects of nanometre size and random distribution is described.

1. Introduction

Silicon crystals grown by the Czochralski (CZ) method or by the Czochralski method in a magnetic field (MCZ) contain supersaturated O atoms that come from the silica crucible. This high concentration of O atoms remains in metastable solid solution during the cooling of as-grown silicon ingots. Although there is a considerable amount of literature concerning the thermal behaviour of oxygen precipitates, the mechanism of their formation in silicon is still an important problem for ultra large scale integrated-circuit fabrication (Claeys & Vanhellemont, 1993). Since the spatial resolu-